

Reprinted from

# Radiation Measurements

---

Radiation Measurements 35 (2002) 127–134

Analysis of the calibration results obtained with Liulin-4J  
spectrometer–dosimeter on protons and heavy ions

Yukio Uchihori<sup>a, \*</sup>, Hisashi Kitamura<sup>a</sup>, Kazunobu Fujitaka<sup>a</sup>, Tsvetan P. Dachev<sup>b</sup>,  
Borislav T. Tomov<sup>b</sup>, Plamen G. Dimitrov<sup>b</sup>, Yura Matviichuk<sup>b</sup>

<sup>a</sup>*International Space Radiation Laboratory, National Institute of Radiological Sciences, Anagawa 4-9-1, Inage, Chiba 263-8555, Japan*

<sup>b</sup>*Solar-Terrestrial Influences Laboratory, Bulgarian Academy of Sciences, Acad. G. Bonchev St. Block 3, Sofia 1113, Bulgaria*

Received 21 May 2001; accepted 24 October 2001



PERGAMON



PERGAMON

Radiation Measurements 35 (2002) 127–134

Radiation Measurements

www.elsevier.com/locate/radmeas

## Analysis of the calibration results obtained with Liulin-4J spectrometer–dosimeter on protons and heavy ions

Yukio Uchihori<sup>a,\*</sup>, Hisashi Kitamura<sup>a</sup>, Kazunobu Fujitaka<sup>a</sup>, Tsvetan P. Dachev<sup>b</sup>,  
Borislav T. Tomov<sup>b</sup>, Plamen G. Dimitrov<sup>b</sup>, Yura Matviichuk<sup>b</sup>

<sup>a</sup>International Space Radiation Laboratory, National Institute of Radiological Sciences, Anagawa 4-9-1, Inage, Chiba 263-8555, Japan

<sup>b</sup>Solar-Terrestrial Influences Laboratory, Bulgarian Academy of Sciences, Acad. G. Bonchev St. Block 3, Sofia 1113, Bulgaria

Received 21 May 2001; accepted 24 October 2001

### Abstract

We are developing a portable dosimeter (Liulin-4J) based on a silicon semiconductor detector for use in measuring the absorbed dose from primary or secondary cosmic rays to astronauts and airplane crews. The dosimeter can measure not only the flux and dose rate, but also the deposited energy spectrum for silicon in per unit time. In order to calibrate the dosimeter, we have carried out exposures at the NIRS cyclotron and HIMAC heavy ion synchrotron facilities. We obtained a detector response function for using in measuring energy deposition and LET. © 2002 Elsevier Science Ltd. All rights reserved.

**Keywords:** Space environment; Dosimeter; Proton; Heavy ion; Calibration

### 1. Introduction

The International Space Station (ISS) is currently being constructed with international collaboration and astronauts have begun to occupy the station for long durations. The environment in the space station is exposed to primary and secondary cosmic rays and the radiation levels inside the ISS are significantly higher than those found on the ground (Fujitaka et al., 1999). In order to monitor the radiation exposure of astronauts, a number of radiation instruments have been developed for use in space. However, it has been recognized that the radiation environment is not uniform inside the spacecraft, but depends on the composition and thickness of shielding materials surrounding the habitable volume (Golightly et al., 1994; Reitz et al., 1997).

One solution to the problem of astronaut dosimetry is for each astronaut to wear a personal radiation monitor. The dosimeter system Liulin-4J has been developed by collaboration between National Institute of Radiological

Sciences (NIRS) and Solar-Terrestrial Influences Laboratory (STIL-BAS) to meet this need. The Liulin-4J system is composed of four Mobile Dosimeter Units (MDU), a Control and Interface Unit (CIU) and an ordinary personal computer (PC) (Fig. 1). This dosimeter system is based on the Liulin-1, 2 and 3M portable dosimeters developed by the STIL-BAS (Dachev et al., 1989, 1999). These systems were successfully used aboard the Russian Mir space station to monitor the radiation field inside the space station. However, the old Liulin dosimeters are not wearable, while the Liulin-4J has not only wearable characteristic but also high performance.

As part of the development effort of the Liulin-4J, we have carried out a series of high energy proton and heavy ion exposures at the NIRS Cyclotron and HIMAC heavy ion accelerators. The purpose of these exposures was to calibrate and characterize the response of the dosimeter system to charged particles of the same types and energies as those encountered in spaceflight. The NIRS cyclotron and HIMAC facilities were developed and have been operated for high energy charged particle and neutral particle cancer therapy. The HIMAC synchrotron facility is one of only a few accelerators worldwide which can accelerate high energy heavy ions (Hirao et al., 1992; Kanai et al., 1999).

\* Corresponding author. Tel.: +81-43-206-3239; fax: +81-43-251-4531.

E-mail address: uchihori@nirs.go.jp (Y. Uchihori).

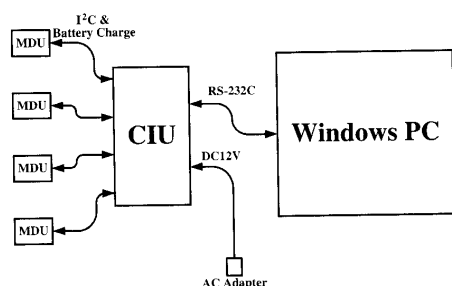


Fig. 1. Schematic drawing of the Liulin-4J System. The mobile dosimeter unit (MDU) has a silicon detector with a thickness of 300  $\mu\text{m}$ . The control and interface unit (CIU) can control up to four MDUs and interfaces with a personal computer.

## 2. Instrument description

Each Liulin-4J MDU has a PIN type silicon semiconductor detector, electric circuits to acquire the data and interface to the PC, and a Li-Ion rechargeable battery. The S2744-08 PIN silicon detector is produced by Hamamatsu Photonics Co.<sup>1</sup> and has an effective area of 10 mm  $\times$  20 mm and a thickness is 300  $\mu\text{m}$ . The uniformity of the thickness is less than 15  $\mu\text{m}$  in the catalogue but it affects 5% of uncertainty of energy deposition of charged particle. An AMPTEK A225F charge amplifier<sup>2</sup> amplifies the signals from the detector with a gain of 5.2 V/pC and peaking time of 2.4  $\mu\text{s}$ . After the amplified signals are shaped by a shaping amplifier (an OP amplifier), the signals are input to a 12-bit Analog-to-Digital Converter (ADC). The ADC is started by output signal from a discriminator and the discriminator discriminates a signal arranged pulse shape of output signal from AMPTEK charge amplifier by a transistor circuit. The converted digital data are read by one PIC16C74 microcontroller<sup>3</sup> and stored as a spectrum in SRAM (512 kbits). Another PIC microcontroller communicates with the first, reads the spectrum and stores it in a flash memory (512 kbytes). The second microcontroller communicates with an external microcontroller in the CIU and sends the stored spectra to the CIU.

The MDU stores histograms, corresponding to the deposited energies of the charged particles in the silicon detector, over a preset sampling time (10–300 s). The histogram can be stored in the flash memory for more than a week if the sampling time is longer than 60 s. The spectrum has 256 channels and the deposited energy range corresponds to  $\sim$  81.3 keV–20.8 MeV in the silicon detector. In the silicon detector, the minimum ionization from a singly charged

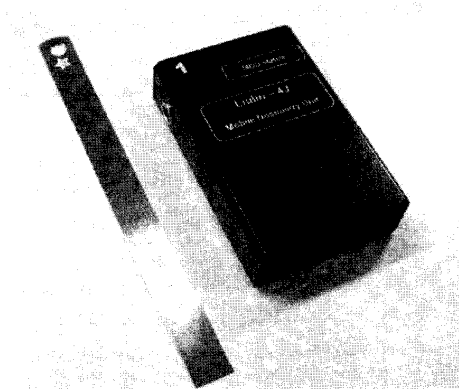


Fig. 2. Photograph of the mobile dosimeter unit (MDU).

particle corresponds to an energy loss of  $\sim$  140 keV. The pedestal value is set less than the 1st channel of the ADC and a pulse which exceeds discrimination level of the discriminator is recorded at the 1st channel.

Each MDU contains a lithium ion rechargeable battery (SONY FP550, 7.2 V and 1500 mA h), which occupies most of the volume in the unit; the MDU can be operated continuously for a period of up to 5 days. The size of the MDU is 94 mm  $\times$  63 mm  $\times$  27 mm and weights 220 g including the battery. The Figs. 2 and 3 show the external appearance of the MDU and a diagram of its electric circuit.

The CIU communicates with the MDU through I<sup>2</sup>C and recharges the battery in the MDU. Here, the I<sup>2</sup>C is one of standard of data transmission with serial signals. Two hours are needed to fully recharge the battery. The CIU communicates with the PC through RS-232C and a user can control the four MDUs through the CIU.

## 3. Cyclotron exposures

Proton and helium beams from the NIRS cyclotron facility (Ogawa et al., 1979) were used for calibration of the energy response of the MDUs; the proton beams were of 30–70 MeV, while the helium beams were of 86–100 MeV. The setup for these experiments is shown in Fig. 4. A MDU was exposed on X-Z capable of rotating in a plane perpendicular to the beam. Stage position and orientation were controlled by a networked computer from outside the irradiation room. The distance between the aluminum window at one end of the beam pipe and the MDU was 10 cm. The center of the silicon detector in the MDU was located at the center of the beam profile. In order to avoid energy loss and energy straggling in other materials, no other detectors or targets were placed in front of the MDU, although an aluminum foil (100  $\mu\text{m}$  thick) was used as a window in

<sup>1</sup> Hamamatsu Photonics K.K., Cat. No. KOTH0002E05.

<sup>2</sup> <http://www.amptek.com/a225f.html>.

<sup>3</sup> <http://www.microchip.com>.

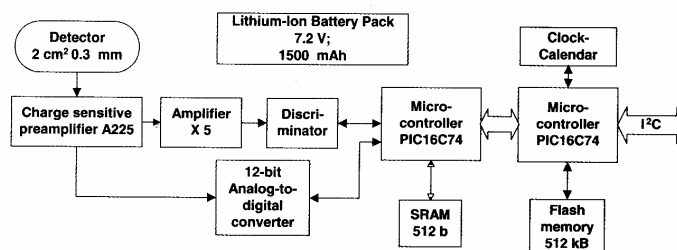


Fig. 3. Block diagram of the MDU. The MDU has one silicon detector, charge sensitive preamplifier, 12-bit analog-to-digital converter, two microcontrollers, SRAM, flash memory, 1500 mA h Li-Ion battery. The MDU can communicate with the CIU through I<sup>2</sup>C and the battery can be recharged when connected to the CIU.

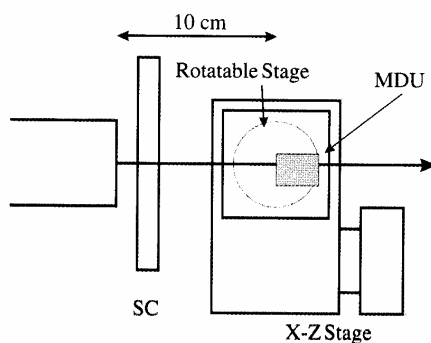


Fig. 4. Top view of setup of the NIRS cyclotron experiments. The MDU was mounted on the X-Z and rotatable stages. The removable plastic scintillation counter (SC) counted the beam intensity before the charged particles irradiated the MDU.

the beam pipe. The beam intensities were adjusted to about  $10^3$  particles per second using a plastic scintillation counter and intensities were confirmed before irradiating the MDU. The beam profiles were tuned to a circular shape (10 mm diameter) and were confirmed using a ZnS fluorescent screen. After the beam tuning, the MDU was irradiated with protons or helium ions. A representative distribution of the deposited energy obtained by MDU-3 for a 40 MeV proton beam is shown in Fig. 5. Several features could be distinguished. First, there was a sharp main peak. This was followed by a small second peak and the background. We confirmed that the second peak corresponded to double particle events (two particles passing through the detector at the same time and producing a single signal) since, when the beam intensity was increased, the population in the second peak became correspondingly larger.

In order to evaluate the results, we compared the experimental measurements with results from the computer sim-

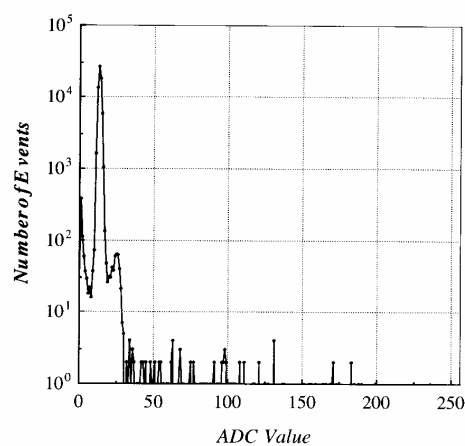


Fig. 5. Representative distribution of the deposited energy in the MDU. This distribution was measured from the 30 MeV proton beam. The main peak is from primary protons. The right side peak at around channel 30 corresponds to the deposited energy of double particle events. This interpretation was confirmed by experiments, in which the beam intensities were decreased and increased.

ulation code GEANT4.<sup>4</sup> The size and arrangement of the detector and the other materials inside and outside of the MDU were reconstructed numerically to simulate the exposure configuration (Fig. 6). The virtual protons were propagated into the reconstructed MDU. Then, the protons were propagated randomly into a region which was 1.5 times larger than the area of the silicon detector.

The distribution of the deposited energy in the MDU is shown in Fig. 7. In these experiments, the silicon detector in the MDU was irradiated at several incident angles in order to confirm whether the deposited energy was proportional to the path length of particles in silicon. Four distributions

<sup>4</sup> <http://wwwinfo.cern.ch/asd/geant4/geant4.html>.

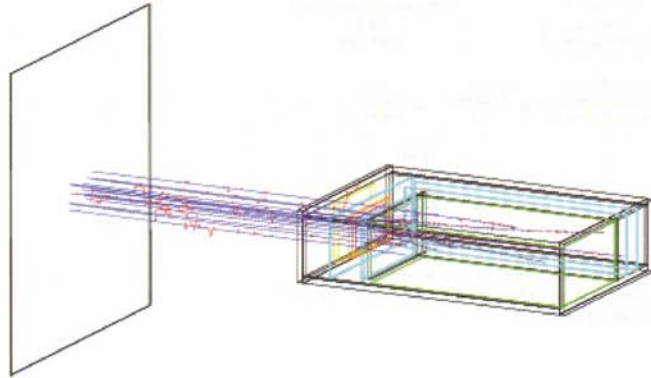


Fig. 6. Simulation results computed by GEANT4 for a proton beam and the MDU. The protons were ejected from the thin aluminum window of the beam pipe, they passed through the air, entered the window of the MDU, and then entered the silicon detector. The battery occupies most of the volume of the MDU.

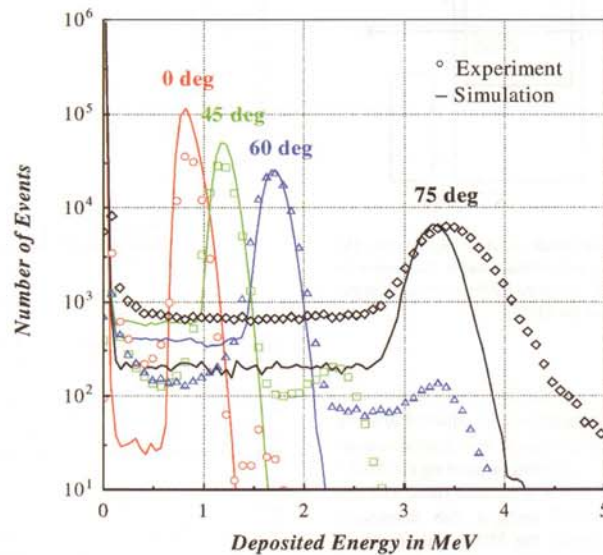


Fig. 7. Comparison of distributions obtained from the cyclotron experiments and the GEANT4 simulation. Four distributions corresponding to deposited energy for  $0^\circ$ ,  $45^\circ$ ,  $60^\circ$  and  $75^\circ$  are shown. The symbols show experiment data and the connecting lines show simulation results for irradiations at these incident angles. The discrepancy of the peak value for  $75^\circ$  between the simulation and experiment data corresponds to a discrepancy of  $1^\circ$  in the  $75^\circ$  irradiation angle.

corresponding to  $0^\circ$ ,  $45^\circ$ ,  $60^\circ$  and  $75^\circ$  are shown. In Fig. 7 the symbols show experiment data and the connecting lines show simulation results for irradiations at these incident angles. Distributions of the experiment and simulation were in good agreement, although the second peak did not appear

in the simulation results because the simulated detector did not have time information and pile up signals could not be represented. As shown in this figure, there were not only primary protons but also other low deposit energy components. We supposed that they were scattering radiations like

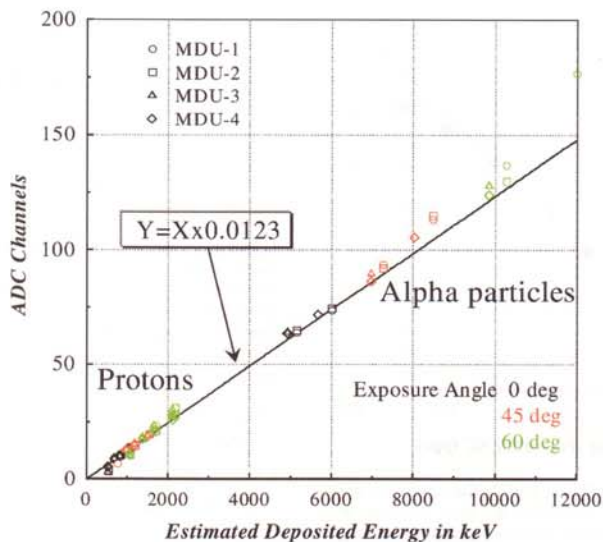


Fig. 8. Summary of results from the NIRS cyclotron experiments. The solid line is the fitted function: Energy = ADC channel no.  $\times$  81.3 keV. The discrepancy between the deposited energies of the alpha particles and ADC channel number at large exposure angles became greater due to the uncertainty in the estimation of deposited energies of the alpha particles.

electrons or gamma rays. Because of these components, there were discrepancies between experiment data and simulated data (i.e. in region less than 0.6 MeV). Especially, for  $75^\circ$ , the shapes of peaks were disagreement but we guess that the scattering component affect the shapes. The scattering radiations were strongly influenced by materials surrounding detector and they might not be considered correctly in the simulation. However, the simulation results represented locations and shapes of peaks of primary protons and they proved that the experiment data were reliable.

Fig. 8 plots the peak values of the distributions of the deposited energies from several experiments that were done with different energies of protons and alpha particles and a line is fitted to the plotted points. Table 1 details the exposure conditions. The estimated deposited energies were calculated using an analytical computer code based on the Bethe–Bloch formula (Salamon, 1980) and taking into account the materials that were in front of the silicon detector. In Fig. 8, results from the exposures made at several angles are included and this data is also in good agreement with the fitted line. In case of alpha particle, the data are a little bit above the fitted line for  $45^\circ$  and  $60^\circ$ . This phenomenon may cause by Coulomb scattering. From the fitted line, we obtained a function to convert ADC channel number to deposited energy in the MDU:

$$\text{Energy} = \text{ADC Channel No.} \times 81.3 \text{ keV.}$$

Table 1

Exposure conditions of the NIRS Cyclotron experiments. The energies of particles, estimated deposited energies in the silicon detector and the individual MDUs used are shown

Date	Particle	Energy (MeV)	Estimated deposited energy* (MeV)	MDU used
April 5, 2000	Proton	70	0.54	1, 2, 3, 4
April 6, 2000	Proton	30	1.09	1, 2, 3, 4
June 28, 2000	Proton	40	0.85	1, 2, 3, 4
June 29, 2000	Alpha	100	5.14	1, 2, 3, 4
July 26, 2000	Proton	30	1.09	1, 2, 3, 4
August 3, 2000	Alpha	86	6.00	1, 2, 4
August 4, 2000	Proton	50	0.70	1, 2, 3, 4
September 13, 2000	Proton	30	1.09	1, 3
November 16, 2000	Proton	40	0.85	1, 3

\*The estimated deposited energies were calculated for the particles which were irradiated with  $0^\circ$  incident angle.

Since the range of the ADC channels was from 0 to 255, the measurable range of the deposited energy in the MDU was from 81.3 keV to 20.8 MeV. The deposited energy range corresponds to LET from 0.27 to 69.3 keV/ $\mu\text{m}$  in silicon if

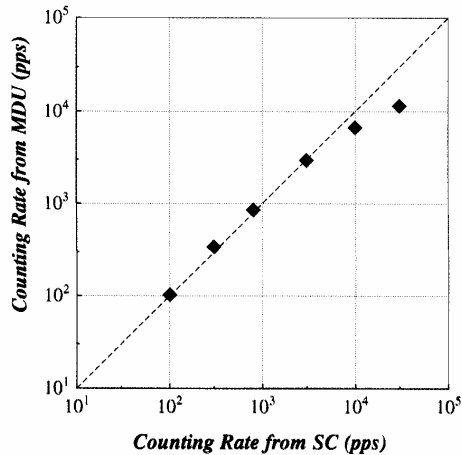


Fig. 9. Confirmation of the efficiency of data acquisition at high count rates. The horizontal axis shows the count rate from the scintillation counter (SC) used as a reference standard, while the vertical axis shows the count rate from the MDU. Above 3000 particles per second, the efficiency of the MDU falls below unity due to dead time in the data acquisition circuitry.

we assume that the particles pass vertically through the disk of the silicon detector.

The efficiency of the data acquisition was also studied. After the beam intensity was tuned against count rate of a scintillation counter, the MDU was irradiated and the detected number of charged particles were counted. In Fig. 9, the horizontal axis is the scintillator count rate used as a reference and the vertical axis is the count rate of the MDU. When the reference count rate was over about 3000 particles per second, the count rate by the MDU was not proportional to the reference count rate due to dead time of the data acquisition circuitry in the MDU. This means that as long as the charged particle flux in the space environment remains below 3000 cps, the MDU is capable of measuring the flux with full efficiency. It also means that the MDU is capable of measuring the charged particle flux in the South Atlantic Anomaly at ISS altitudes (Dachev et al., 1998).

#### 4. Heavy ion experiments

In order to investigate the response of the Luilin-4J to particles that produce large energy deposition in the detector, exposures were made using a number of heavy ions. Results from exposures of carbon and neon ions (400 MeV/u) are reported. The beam profiles were adjusted to square shapes with 20 mm side lengths and confirmed using a ZnS fluorescence screen and a position sensitive silicon detector prior to exposure of the MDUs. The beam intensity was ad-

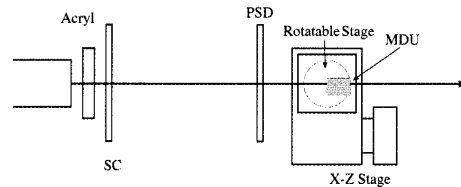


Fig. 10. Top view of the exposure setup used in the HIMAC experiments. The MDU was mounted on the  $X$ - $Y$  and rotatable stages. Both stages were controlled from outside the irradiation room. The position sensitive silicon detector (PSD) was set in front of the MDU to confirm beam profiles. The thin plastic scintillation counter (SC) monitored the beam intensity. The acrylic targets were placed immediately in front of the beam pipe during the fragmentation experiments.

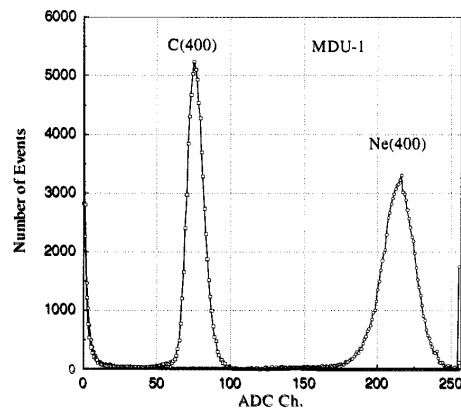


Fig. 11. The distribution of ADC channel number corresponding to the deposited energies in the MDU, for primary carbon and neon ions. The distributions which are got from experiments for carbon and neon ions are superposed in this figure.

justed to 1000 particles per spill. The setup of the HIMAC exposures are shown in Fig. 10. In order to measure the beam intensity, a 50  $\mu\text{m}$  thick, plastic scintillation counter (SC) was placed immediately in front of the beam pipe. The MDUs were mounted on a  $X$ - $Y$  stage and a rotatable stage, both controlled by a personal computer and this computer was operated outside of the irradiation room. The MDU was located 1.5 m from the end of the beam pipe.

For direct exposure of the MDU to carbon and neon ions, the deposited energies in 300  $\mu\text{m}$  thick silicon were estimated, using a computer calculation (Salamon, 1980), to be  $\sim 6.1$  and  $\sim 17.3$  MeV. Fig. 11 shows the observed distributions in ADC channel number of the carbon and neon ions, corresponding to the deposited energies in the silicon detector. The distributions from carbon and neon exposures are

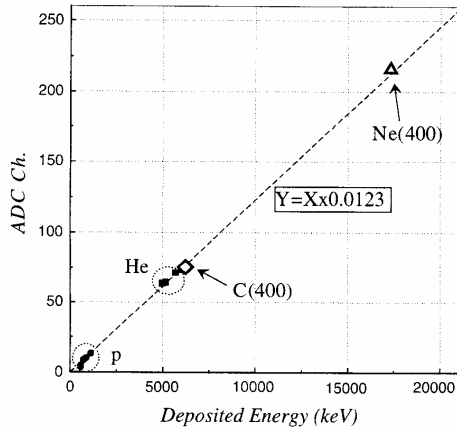


Fig. 12. The relation of estimated deposited energy in the silicon detector in the MDU and ADC channels. The data for irradiation at  $0^\circ$  incident angle are shown. Carbon and neon data were in good agreement with the formula  $ADC = \Delta E \times 0.0123$ , which was obtained from the cyclotron experiments.

superposed. Formula energy =  $ADC \times 81.3$  keV obtained from Fig. 8 shows good agreement with the heavy ions exposures (Fig. 12). Here, the resolutions of the deposited energy distribution were  $\delta(\Delta E)(fwhm)/\Delta E = 17\%$  and  $12\%$ , respectively.

In order to measure the deposited energies from lighter ions, an acrylic plate (10 mm thick) was inserted in front of the MDU to produce projectile fragments in the beam. Fig. 13 shows the deposited energy distribution of the fragment ions produced by the acrylic plate. Fragments could be distinguished from the deposited energy distribution of the primary ions. In order to confirm that the peaks in this distribution corresponded to light ions, the average deposited energies of the light ions were calculated analytically. It was assumed that every ion underwent energy loss only through ionization and that there was no energy loss from nuclear interactions in the acrylic plate. We also assumed that all fragment ions were produced at the center of the thickness of the acrylic plate. The estimated deposited energies of the projectile fragments are indicated in Fig. 13 by arrows. For neon or heavier ions there was a slight disagreement between the measurement and the estimates, while for lighter ions measurement and calculation were in good agreement.

Since the MDUs were set on an X–Y stage, the position of the MDU could be changed, and the incident angle relative to the production point of the fragments could also be changed. Thus, we were able to determine the distribution of projectile fragments as a function of angle. Fig. 14 shows the distribution of the deposited energy for projectile fragments at different incident angles. Due to differences in incident angle, the distribution of fragment ions is different

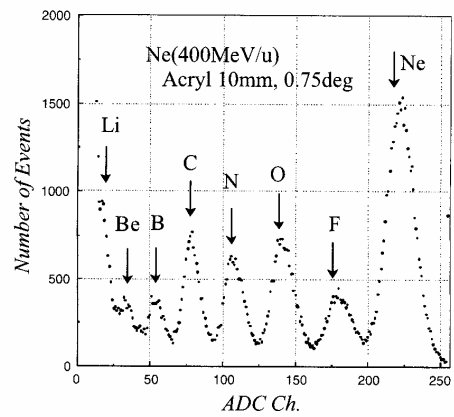


Fig. 13. Deposited energy distribution obtained from projectile fragments. The peaks in the spectrum correspond to ions lighter than the primary ions. The MDU was situated  $0.75^\circ$  relative to the beam line direction. The arrows indicate estimates of deposited energies for each fragment ion.

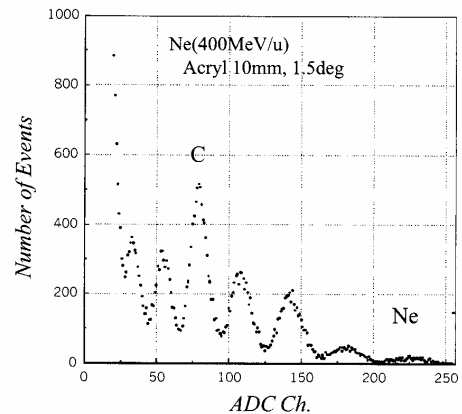


Fig. 14. Deposited energy distribution obtained in the projectile fragment ion beam. The peaks in the spectrum correspond to ions lighter than the primary ions. The MDU was situated  $1.5^\circ$  relative to the beam line direction. Comparisons with Fig. 13 show that the distribution of each ion is not the same.

from that seen in Fig. 13. It should be noted that, in Fig. 13, the detector is hit by primary beams and much neon ions were observed than Fig. 14. With these distributions, we can use this information to estimate the double differential cross section of each fragment ion; these results will be reported elsewhere.

## 5. Conclusions

The mobile dosimeter system Liulin-4J is being developed by a joint Bulgarian and Japanese collaboration. Calibration of the Mobile Dosimeter Units has been carried out using proton and heavy ion beams from the NIRS Cyclotron facility and the HIMAC heavy ion synchrotron facility at NIRS.

In these experiments, we determined that the response of the MDU is in good agreement with calculated estimates of deposited energy in the silicon detector. A function to convert ADC channel number to deposited energy in silicon was obtained. In addition, we determined that the maximum counting rate of the MDU without missing events was about 3000 events per second. This counting rate is higher than the maximum counting rate necessary to measure trapped proton flux at ISS altitudes in the South Atlantic Anomaly. Heavy ion experiments also confirmed that the dosimeter can measure the fragmentation of heavy ions and it was established that the energy resolution of the MDU is sufficiently fine to distinguish the charge peaks of the individual fragment ions.

## Acknowledgements

We thank member of the operation team for the NIRS cyclotron facility. A part of this study was performed as the Research Project with Heavy Ions at NIRS-HIMAC. We are grateful to all members of HIMAC for their support. The authors also want to thank Dr. Eric Benton for carefully reading this manuscript.

## References

- Dachev, Ts.P., Matviichuk, Yu.N., Semkova, J.V., Koleva, R.T., Boichev, B., Baynov, P., Kanchev, N.A., Lakov, P., Ivanov, Ya.J., Tomov, B.T., Petrov, V.M., Redko, V.I., Kojarinov, V.I., Tykva, R., 1989. Space radiation dosimetry with active detection's for the scientific program of the second Bulgarian cosmonaut on board the MIR space station. *Adv. Space Res.* 9 (10), 247.
- Dachev, Ts.P., Semkova, J.V., Matviichuk, Yu.N., Tomov, B.T., Koleva, R.T., Baynov, P.T., Petrov, V.M., Shurshakov, V.V., Ivanov, Yu., 1998. Inner magnetosphere variations after solar proton events. Observations on MIR space station in 1989–1994 time period. *Adv. Space Res.* 22 (4), 521–526.
- Dachev, Ts.P., Tomov, B.T., Matviichuk, Yu.N., Koleva, R.T., Semkova, J.V., Petrov, V.M., Benghin, V.V., Ivanov, Yu.V., Shurshakov, V.A., Lemaire, J.F., 1999. Solar Cycle variations of MIR radiation environment as observed by the LIULIN dosimeter. *Radiat. Meas.* 30, 269–274.
- Fujitaka, K., Majima, H., Ando, K., Yasuda, H., Suzuki, M. (Eds.), 1999. Risk evaluation of cosmic-ray exposure in long-term manned space mission. Proceedings of the International Workshop on Responses to Heavy Particle Radiation, Chiba, July 9–10, 1998.
- Golightly, M.J., Hardy, K., Quam, W., 1994. Radiation dosimetry measurements during U.S. Space Shuttle Missions with the RME-III. *Radiat. Meas.* 22 (1), 25–42.
- Hirao, Y., Ogawa, H., Yamada, S., Sato, Y., Yamada, T., Sato, K., Itano, A., Kanazawa, M., Noda, K., Kawachi, K., Endo, M., Kanai, T., Kohno, T., Sudou, M., Minohara, S., Kitagawa, A., Soga, F., Takada, E., Watanabe, S., Endo, K., Kumada, M., Matsumoto, S., 1992. Heavy ions synchrotron for medical use-HIMAC project at NIRS-JAPAN. *Nucl. Phys. A* 538, 541c–550c.
- Kanai, T., Endo, M., Minohara, S., Miyahara, N., Koyama-Ito, H., Tomura, H., Matsufuji, N., Futami, Y., Fukumura, A., Hiraoka, T., Furusawa, Y., Ando, K., Suzuki, M., Soga, F., Kawachi, K., 1999. Biophysical characteristics of HIMAC clinical irradiation system for heavy-ion radiation therapy. *Int. J. Radiat. Oncol. Biol. Phys.* 44 (1), 201–210.
- Ogawa, H., Yamada, T., Kumamoto, Y., Sato, Y., Hiramoto, T., 1979. Status report on the NIRS-CHIBA isochronous cyclotron facility. *IEEE Trans. Nucl. Sci.* NS-26 (2), 1988–1991.
- Reitz, G., Beaujean, R., Kopp, J., Leicher, M., Strauch, K., Heilmann, C., 1997. Results of dosimetric measurements in space. *Radiat. Prot. Dosimetry* 70, 413–418.
- Salamon, M.H., 1980. A range-energy program for relativistic heavy ions in the region  $1 < E < 3000$  MeV/amu. LBL Report 10446, LBL, Berkeley.